2013

The effect of mixing methods on the dispersion of carbon nanotubes during the solvent-free processing of multiwalled carbon nanotube/epoxy composites

The Effect of Mixing Methods on the Dispersion of Carbon Nanotubes During the Solvent-Free Processing of Multiwalled Carbon Nanotube/Epoxy Composites

Murari L. Gupta,[1] Stefanie A. Sydlik,[2] Jan M. Schnorr,[2] Dong Jin Woo,[3] Sebastian Osswald,[3] Timothy M. Swager,[2] Dharmaraj Raghavan[1]

[1]Department of Chemistry, Howard University, Washington, District Of Columbia 20059

[2]Department of Chemistry and Institute for Soldier Nanotechnologies, Massachusetts Institute of Technology, Cambridge, Massachusetts 02139

[3]Department of Physics, Graduate School of Engineering and Applied Science, Naval Postgraduate School, Monterey, California 93943

Correspondence to: D. Raghavan (E-mail: draghavan@howard.edu)

Received 9 August 2012; revised 16 October 2012; accepted 22 October 2012; published online 10 December 2012
DOI: 10.1002/polb.23225

ABSTRACT: Several solvent-free processing methods to disperse multiwalled carbon nanotubes (MWCNTs) in bisphenol F-based epoxy resin were investigated, including the use of a microfluidizer (MF), planetary shear mixer (PSM), ultrasonication (US) and combinations. The processed mixture was cured with diethyl toluene diamine. Three complimentary techniques were used to characterize the dispersion of the MWCNTs in cured composite samples: optical microscopy, micro Raman spectroscopy, and scanning electron microscopy (SEM). For sample MF + PSM, optical micrographs and Raman images showed reduced agglomeration and a homogeneous distribution of MWCNTs in the epoxy matrix. SEM analysis of fractured specimen after tensile testing revealed breakage of nanotubes along the fracture surface of the composite. A comparison of the MWCNT dispersion in the epoxy samples processed using different methods showed that a combination of MF and PSM processing yields a more homogeneous sample than the PSM or US + PSM processed samples. Mechanical testing of the composites showed about 15% improvement in the tensile strength of samples processed by the MF + PSM method over other methods. Thermogravimetric analysis (TGA) results showed a small decrease in the onset degradation temperature for poorly dispersed samples produced by PSM compared with the well-mixed samples (MF + PSM). These results strongly suggest that the MF + PSM processing method yield better-dispersed and stronger MWCNT/epoxy composites.

J. Polym. Sci., Part B: Polym. Phys. **2013**, *51*, 410–420

KEYWORDS: composites; fillers; fracture; mechanical properties; multiwalled carbon nanotubes; nanotechnology

INTRODUCTION Thermoset resins represent an important class of engineering polymers that account for nearly 20% of the polymers market, which encompasses composites, adhesives, and coatings.[1] Among the most prevalent engineering thermosets, epoxy resins have been widely used because of their excellent environmental and dimensional stabilities. In addition, epoxies exhibit good bulk properties such as strength, modulus, hardness, and adhesion to fillers. However, resins of this class can be brittle and show poor resistance to crack growth due to their high cross link density and amorphous characteristics. To address the brittle characteristics of the crosslinked resin, generally glass or carbon fibers at high weight percent (wt %) have often been used as reinforcing material.[2,3] Fiber reinforcement has proven to be effective in improving the fracture toughness of the composite. For maximum reinforcement, the optimal loading of the fibers typically falls in the range of 30–60 wt %, which can adversely impact the weight of the composite. Nanofillers have received much attention from the scientific and technological community as replacement for conventional fibers in fiber reinforced epoxy resin.[4–7] This is because nanofiller dispersed polymer composites can potentially show dramatic improvement in mechanical, thermal, and electrical properties upon addition of few wt % of nanofillers to a polymeric resin, and more importantly without a significant weight penalty. Potential applications of carbon nanotube-filled nanocomposites include coatings, sensors, probes, energy storage devices, field emission displays, and structural materials, such as lightweight vehicles, aircrafts, civil constructions, sports equipments, marine, and military hardware.[8–12] For structural applications, typically 0.5 wt % loading of multiwalled carbon nanotubes (MWCNTs) in epoxy resin is considered adequate to produce high impact-resistant structures.[13–18] However, poor dispersion of MWCNTs in polymer or host matrix such as epoxy can limit the

Additional Supporting Information may be found in the online version of this article.

translation of the excellent mechanical properties of MWCNTs into the MWCNT-filled nanocomposites.[19] MWCNTs exhibit strong intertube interactions and are thus prone to poor dispersion and agglomeration in epoxy. An approach to address this challenge is the covalent or noncovalent functionalization of MWCNTs to improve their interaction with solvents and/or polymers leading to better dispersibility.[20] Several chemical functionalization methods have been studied including covalent side-wall functionalization, noncovalent functionalization, oxidation by nitric acid-etching, and nitrene chemistry.[12,17,21–28] Despite the success in functionalizing MWCNTs with desired chemical groups, engineering good dispersion and orientation of functionalized MWCNTs in resin remains a challenge. When MWCNTs are well dispersed, they form networks in the polymer matrix, and the networks are responsible for enhanced reinforcement of polymer composites containing MWCNTs.

Another approach to overcome bundling of MWCNTs is to develop effective mixing procedures.[29] The "as-produced" MWCNTs show poor dispersion within the polymer matrix because of high cohesive strength. To overcome this challenge, nanotubes are vigorously mixed in a solvent prior to their addition to the epoxy or a solvent-diluted epoxy.[30] The selection of solvent is based on polymer miscibility, MWCNT dispersibility in the solvent, and the ease with which solvent can be evaporated. The effect of solvent on the MWCNT dispersion has been previously reported by Song et al., who used an ultrasonication (US) mixing method.[19] Although improved dispersion can be achieved by using solvent, the presence of trace amounts of residual solvent and/or entrapped bubbles in the final composite, despite application of vacuum to the mixture, can have a negative effect on the overall thermal and mechanical properties of the nanocomposite.[31] Proper selection of solvent and the use of an efficient solvent removal method is essential when considering solvent-based methods to disperse MWCNTs in a polymer matrix.[31]

Alternatively, solvent free processing methods (e.g., stirring, kneading, extrusion, shear mixing,[32] high pressure homogenizer,[18] calendaring, or three-roll mill[33]) have been studied to formulate homogenous MWCNT/polymer composites. While there is a substantial amount of literature available for three-roll mill and US processing methods; limited literature is available on the use of high shear mixing methods, such as planetary shear mixing and microfluidics (MF), to deagglomerate CNTs in polymer nanocomposites.[15,17,18,34] In US, a pulsed ultrasound wave causes generation and collapse of submicron-sized bubbles of the resin mixture and thus deagglomeration of MWCNTs in the polymer matrix. However, processing of MWCNTs and polymer mixture using microfluidizer (MF) involves the fluid flowing at high velocities through microchannels of various geometries, and exposing the mixture to high shear stresses. The applied pressure and the channel geometry in MF control the fluid velocities inside the microchannels, and hence the extent of MWCNTs deagglomeration.[35] MF processors use unique microchannel design which offers the flexibility to generate high shear rates by subjecting the nanomaterial along with epoxy resin to high pressure conditions. Based on the literature data from Microfluidics, MF can generate shear rates of more than 10^7/s as compared with 5×10^5/s in roll mill and 7×10^5/s in high shear homogenizer.[36] Apart from MF ability to generate high shear rates, MF processors also lends itself for different scales of processing. While in the planetary shear mixer, the MWCNT/polymer mixture is rotated at very high radial velocity under high shear mixing conditions so as to achieve deagglomeration of nanotube bundles. Kasaliwal et al. describe the deagglomeration mechanisms of MWCNTs in polymer matrix as a function of mixing conditions and processing protocols.[37] The two modes of deagglomeration of MWCNT bundles are erosion and rupture. The rupture mode of dispersion becomes prominent when the large agglomerates are broken down to smaller aggregates in a short time period such as in the case of MF where the MWCNT/epoxy mixture is force-fed through a microchannel under very high pressure in a short time period (about 30 s). The erosion mode of dispersion mechanism is prominent when large agglomerates of MWCNTs erode from the bundle and dispersion occurs gradually in the matrix over a longer period of time. For example, slow dispersion takes place in US (about 1 h dispersion time) and planetary shear mixing (about 30 min dispersion time). Planetary shear mixing (PSM), MF, and combination methods provide high shear processing alternatives to solvent based methods in effectively dispersing CNTs in epoxy matrix.

It is important to assess the effectiveness of mixing procedures in dispersing MWCNTs in the polymer matrix. Generally, characterization techniques, which encompass morphological measurements over length scales in the micrometer down to the nanometer range, are sought for evaluating dispersion of MWCNTs in epoxy samples. Optical microscopy and Raman imaging are conventionally used to evaluate the dispersion of MWCNTs aggregates in a polymer matrix on the micro-scale (>1 μm), while scanning electron microscopy (SEM), transmission electron microscopy (TEM), and/or atomic force microscopy (AFM) are used to measure dispersion, alignment, and local concentration gradients of the MWCNTs in polymer matrix in the submicrometer range (<1 μm).[38] Although optical microscopy is inadequate for submicrometer-scale characterization, it is fast, nondestructive, and provides a preliminary assessment of the overall distribution of MWCNT agglomerates present in the processed nanocomposites. However, SEM and AFM allow for the characterization of nanocomposite morphology at the submicrometer scale, but these techniques provide only surface information unless the cross-sections of fractured specimen are observed. More recently, Raman spectroscopy has been shown to be a powerful tool for the characterization of CNT/polymer composites. Particularly, Raman mapping and Raman imaging were used as complementary tool to optical microscopy to evaluate the dispersion of the CNTs in the polymer matrix at the micrometer scale. Most of the previous studies have used the Raman features of the CNTs to analyze the stress transfer in polymer composites.[39–43] Park and Lillehi reported that a

combination of optical microscopy and Raman imaging provides more accurate information of CNT dispersion at several length scales.[38] Similarly, Du et al. used the intensity distribution under the sampling volume around the second order graphitic band, G' band (2700 cm^{-1}), of reduced single-walled carbon nanotubes/polymethyl methacrylate nanocomposites to obtain Raman maps of CNT dispersion in epoxy matrix.[44] In this study, we explored a combination of the above techniques to assess the dispersion of MWCNTs in epoxy composites prepared via solvent-free processing protocols.

Although most of the studies found in literature focused on the use of solvents to predisperse MWCNTs before mixing with epoxy resin, this study compares microprocessing (MF), high shear homogenization (planetary shear mixer), US, and combinations thereof, to disperse MWCNTs in epoxy resin in the absence of solvent. MF processor utilizes state of the art micro channel configuration as outlet. The pre-mixed MWCNT/epoxy mixture is pumped at very high pressure (20,000 psi) in the processor to deagglomerate MWCNT bundles and to disperse the MWCNTs in the epoxy resin. A schematic of the MF processor is shown in Figure 1(a).

In PSM, the mixing container rotates in opposite direction to the central rotating shaft at much lower speed (800 rpm) than the central rotating drum (2000 rpm), thus generating high shear forces in the container, which homogenizes the filler in the host polymer or epoxy matrix. A schematic of the PSM is shown in Figure 1(b) (adapted from Thinky Mixer literature).[45] Optical microscopy, Raman microspectroscopy, and SEM were used to characterize the morphology and homogeneity of MWCNTs/epoxy nanocomposite as they give complimentary information about the state of nanotubes dispersion in the polymer matrix.

To make the comparison meaningful (evaluate CNT dispersion) between samples processed using various methods, the loading of MWCNT in the epoxy nanocomposite was kept constant at 0.5 wt %. Although we worked at 0.5 wt % CNT concentration, it is common to find nanocomposite literature where the CNT content ranged from 0.1 to 1 wt %. In fact, Gojny's 2004 work used only 0.1 wt % CNT to show the effectiveness of processing method in dispersing CNTs.[14] Furthermore, Gonjalez et al. studied the noncovalent wrapping of CNT with block copolymer and found that 0.5 wt % concentration of noncovalently wrapped CNTs provided the highest improvement in the mechanical properties of CNT/epoxy nanocomposites.[15] This report motivated us to choose 0.5 wt % CNT concentration in our studies to investigate the effect of processing methods.

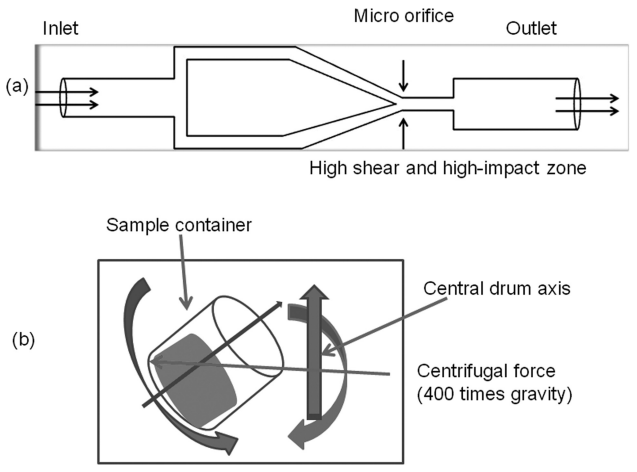

FIGURE 1 Schematic presentation of (a) Microfluidizer and (b) Planetary shear mixer* (*adapted from Thinky Mixer literature).

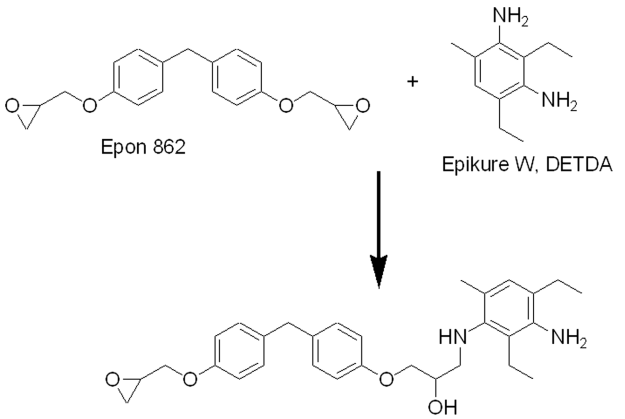

SCHEME 1 Curing reaction of Epon 862 and DETDA curing agent (Epikure W).

EXPERIMENTAL

Materials

Epon 862 and Epikure curing agent W were supplied by Momentive Chemicals, USA and were used as received. Pristine multiwall carbon nanotubes were purchased from Sigma Aldrich USA (carbon > 95%, O.D. × L 6–9 nm × 5 μm, number of walls were 3–6, median tube diameter was 6.6 nm) and were used as received. The chemical structures and reaction of Epon 862 and Epikure curing agent W are shown in Scheme 1.

MF processing was conducted by Microfluidics Inc, Newton, MA. Planetary shear mixer also known as "Thinky Mixer" (atmospheric pressure type) ARE 310 was provided by Thinky Corporation USA. Branson Sonic Dismembrator was used for US.

Methods

The general description of preparing MWCNTs/epoxy nanocomposite using various processing methods is shown in Figure 2.

Planetary Shear Mixer Mixing Method

To 9.95 g Epon 862 epoxy resin weighed in the polypropylene container, 0.05 g pristine MWCNTs was added. Then the 35 mL container was sealed and mounted in the ARE 310 Thinky Mixer. The mixing speed was maintained at 2000 rpm and the CNT and epoxy mixture was homogenized for 30 min. The sample was cured in a programmable oven according to the curing protocol described in later section.

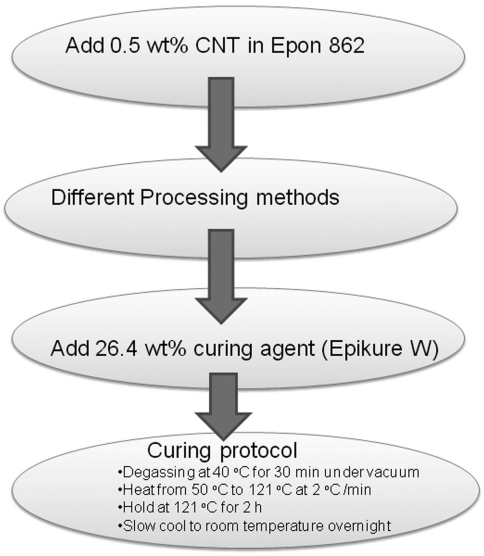

FIGURE 2 Process flow chart of nanocomposite preparation method.

MF Mixing Method

Initially, 99.5 wt % epoxy and 0.5 wt % pristine MWCNTs were pre-mixed using high speed IKA Rotastat for 5 min at 20,000 rpm and at 65 °C to reduce the viscosity of epoxy so as to avoid clogging of microchannel during MF processing. M110S MF was used in microfluidic processing of premixed MWCNTs/epoxy sample. MF processing trials were performed using the H30Z (200 μm) IXC at 15,000 psi and the H10Z (100 μm) IXC at 20,000 psi. Since, the study by Microfuidics[46] reported that MF processing can reduce the CNT length when the composite mixture is passed multiple times (about 5–20 passes) through the MF processor, we subjected the mixture to a maximum of two passes to process the MWCNT/epoxy samples so as to minimize MWCNT length reduction. For one batch of samples, the mixture was allowed to pass twice through 200 μm channel (bigger bore channel), while for the other batch of samples, the mixture was allowed to pass once through 100 μm channel (smaller bore channel). Optical microscopic images were collected of the mixture before and after passage through the MF processor. These studies were conducted to demonstrate the role of processing conditions (i.e., pressure and microchannel diameter) on the dispersion of MWCNTs in epoxy specimen. A portion of the dispersed sample was collected and cured as per the curing protocol and the remaining portion of the MF processed sample was further subjected to dispersion in planetary shear mixer as described in the planetary shear mixing method mentioned above to get MF + PSM processed sample. The MF + PSM processed samples were also cured as per curing protocol described in later section.

Ultrasonicator Mixing Method

The 0.05 g MWCNT/9.95 g epoxy mixture was sonicated with a high-powered sonic dismembrator (Branson) for 30 min. During US, the power of sonication was gradually raised while maintaining the temperature of the mixture at 35 °C by placing the reaction vessel in a water jacket. The water jacket acted as a heat sink to avoid excessive heat buildup in the sonication vessel. A considerable amount of froth forms and there is a decrease in viscosity during sonication. After sonication, the vessel was allowed to equilibrate to room temperature and the sonicated mixture was placed in a vacuum oven at 40 °C for 30 min. A portion of the US processed sample was saved for curing and the other portion was subjected to planetary shear mixer processing as described above. The US + PSM processed sample was degassed at 40 °C under vacuum for 30 min and then cured in the programmable oven as described in the curing protocol below.

Curing Protocol

To 0.5 wt % pristine MWCNT/epoxy mixture processed by various mixing methods, 26.4 wt % curing agent W was added and hand mixed vigorously. The mixture was degassed under vacuum at 40 °C for 30 min. A few drops of the degassed mixture were spin-coated on glass coverslips and silicon wafers to characterize the dispersion of MWCNTs in epoxy sample by optical microscopy and micro Raman spectroscopy, respectively. The bulk of the MWCNTs/epoxy mixture was poured into dog-bone shaped molds of silicon rubber and placed for degassing at 40 °C in vacuum oven for 30 min and then placed in a programmable oven (Thermofisher). Curing was initiated by ramping the oven temperature from room temperature to 121 °C at 2 °C/min and holding the sample at 121 °C for 2 h followed by slow cooling of the sample to room temperature overnight. Similar protocol has been reported to cure epoxy nanocomposites.[43,44] The mechanical properties of the dog bone samples were characterized by performing tensile test measurements.

Optical Microscopy

Keyence Digital Microscope VHS 1000 was used to screen the spin coated MWCNT/epoxy samples in transmission light mode. A 1000× objective was used to collect individual images and develop a montage of the sample. A minimum of four measurements were recorded for each of the processing conditions, unless otherwise stated. The images were processed by using an automated batch program (NIH's Image J program) and the images were thresholded to determine the number and size of MWCNTs aggregates in each of the processed sample.

Raman Spectroscopy and Raman Imaging

Raman spectra were recorded using an in Via Confocal Raman Microspectrometer (Renishaw, UK) with a 780-nm excitation laser (2 mW with 20× objective) and a 1200 L/mm grating. Data analysis and curve fitting were performed using Renishaw's Wire 2.0 software. For Raman imaging of the composites, dog bone samples were broken apart along the bone axis, mounted in a secondary epoxy matrix, polished, and rinsed with ethanol to obtain a clean, flat surface. Neither the use of a secondary epoxy nor the polishing process was found to interfere with the Raman analysis.

Tensile Testing

The molding process produced dog-bone specimens were ~25 mm (length) by 4 mm (gauge width) by 1.8 mm (thickness) in size. Tensile experiments were conducted on an MTI

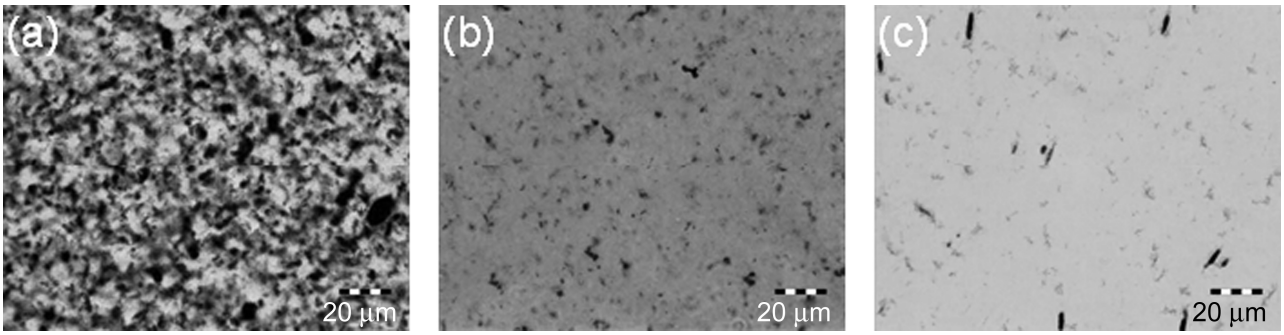

FIGURE 3 Optical microscope images of uncured liquid mixtures of pristine MWCNT/epoxy nanocomposite (a) unprocessed; (b) MF Processed through H30Z (200 μm) IXC at 15,000 psi; and (c) MF processed through the H10Z (100 μm) IXC at 20,000 psi.

tensile tester equipped with 10 kN load cell capability with strain gauges. The experiments were conducted at room temperature using a cross-head speed of 2.54 mm/min. A 0.2 N pre-load was applied to prevent slippage of test specimen. The stress-strain curves were recorded for about seven specimens of each composition.

Scanning Electron Microscopy

Tensile fractured samples were mounted on an aluminum stub; Au-Pd was deposited on the fractured surface and observed using Jeol JSM 7600F Field Emission SEM. A 10 kV accelerating voltage and secondary electron mode was used with a working distance of 8 mm. Micrographs were collected at several magnifications to map MWCNT agglomeration and describe the mode of nanotube fracture in the epoxy nanocomposites.

Thermogravimetric Analysis

A Seiko nanotechnology thermogravimetric analysis (TGA) instrument was used to study the influence of MWCNT dispersion on thermal degradation of the nanocomposites. Samples were postcured at 177 °C for 2 h and then slow cooled to room temperature before analysis by TGA. A post-cured sample (8–12 mg) was heated from room temperature to 100 °C at a heating rate of 10 °C/min and kept for 30 min; then ramped from 100 to 450 °C at a rate of 10 °C/min and then cooled back to room temperature at a rate of 10 °C/min. TGA was performed under nitrogen atmosphere at a purge rate of 100 mL/min.

RESULTS AND DISCUSSION

Optical Microscopy

Optical microscopy has been previously used as a fast screening technique to study the deagglomeration and dispersion of nanomaterials (i.e., nanoclays and carbon nanotubes) in epoxy matrix.[17,37] However, the technique has not been adopted to quantify deagglomeration of MWCNTs in epoxy. In this study, we used the National Institute of Health's (NIH) Image J program to quantify the agglomerate number and size distribution in MWCNT/epoxy nanocomposties.

Figure 3 presents optical microscopic images of uncured (a) unprocessed, (b) MF processed through the H30Z (200 μm) IXC channel at 15,000 psi, and (c) MF processed through the H10Z (100 μm) IXC channel at 20,000 psi, pristine MWCNT/epoxy mixtures. The images shown are from representative regions of droplets of the liquid mixture placed on a glass coverslip. We note that even within different regions of the liquid mixture, there may be small variation in the deagglomeration of nanotubes. Visual inspection of the optical images shows that the MWCNT dispersion varies between unprocessed and processed liquid mixtures. Overall, there were large agglomerates ($>$145 μm^2) in the unprocessed sample. In contrast, a considerable amount of smaller aggregates ($<$2.5 μm^2) were noticed throughout the image in the sample that was passed through bigger bore channel (200 μm) during MF processing. Similarly, smaller aggregates were noticed in the sample that was passed through the smaller bore channel (100 μm) during MF processing. In addition, the images of MF processed samples that passed through smaller bore channel showed that there were thin, oriented clusters of nanotubes (about 10 μm long and 1 μm wide) distributed throughout the epoxy matrix. This indicates that the oriented nanotube clusters were detached from the bundles and are distributed throughout the matrix of MF processed samples, while in the unprocessed sample the bundles largely remain intact and exhibit macrophase separation.

Optical microscopy results showed that there was no significant variation in the MWCNT dispersion in MWCNT (0.5 wt %)/epoxy mixture that was subjected to IKA Rotastat preprocessing and that passed through MF of bore channel H10Z (100 μm) IXC at 20,000 psi or MF bore channel H30Z (200 μm). Therefore, the liquid mixture that was processed through MF bore channel H30Z (200 μm) was used for a comparative study of the effect of various processing methods on the quality of nanotube dispersion in cured sample.

Next, we have further compared the optical microscopic images of cured samples processed using various methods. Figure 4 represents the montage of cured (a) US, (b) PSM, (c) US + PSM, (d) MF, and (e) MF + PSM processed MWCNT/epoxy samples. A comparison of the images shows a considerable degree of variability in the extent of deagglomeration and dispersion of MWCNTs in the epoxy matrix depending on the mixing method employed. For example, in the US processed sample, there are many large aggregates

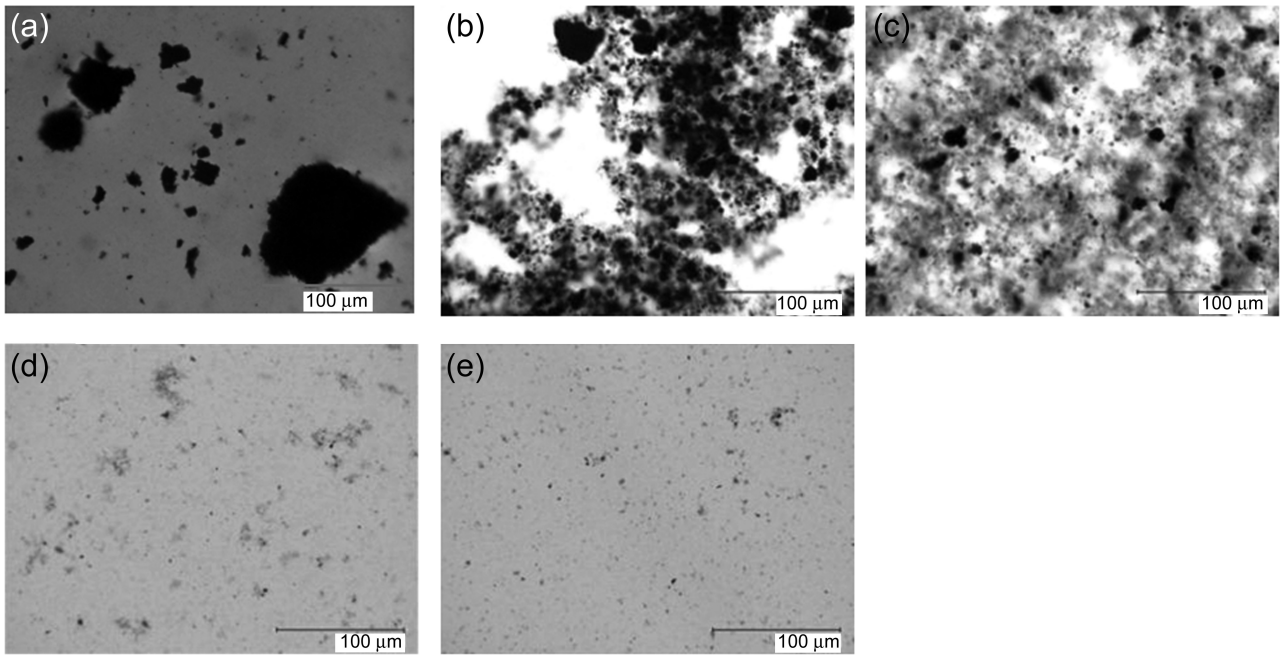

FIGURE 4 Effect of processing methods on dispersion of pristine MWCNT in epoxy resin (a) US; (b) PSM; (c) US + PSM; (d) MF; and (e) MF + PSM.

and some small aggregates, while in PSM processed sample there are fewer large particles and many small particles. The US + PSM processed sample exhibits many small particles, and in MF and MF + PSM processed samples, there are fewer small particles as observed by optical microscopy. We performed a more detailed quantitative image analysis using an automated batch program (NIH's Image J software). The image was first "color thresholded" and then analyzed to determine agglomerate areas in a range from 2.5 to 145 μm^2. The agglomerate number and size (as defined by area) were plotted in Figure 5 for different processing methods. A minimum of four images of each processed sample was used for quantification purposes with error bars showing standard deviation in the different areas of the processed samples. MF + PSM processed sample has the least number of smallest size (2.5 μm^2) agglomerates (4) while US has the maximum number (9) of larger agglomerates (145 μm^2). PSM processing of the CNT/epoxy mixture generates a considerable number (35) of smaller (2.5 μm^2) agglomerates and a fewer number (2) of larger (145 μm^2) agglomerates, while the combination of US + PSM processing generates a largest number (62) of smaller (2.5 μm^2) agglomerates with not so noticeable amount of larger agglomerates. A word of caution, it is difficult to discern from the optical images of MF + PSM combination processed samples whether there are additional smaller clusters of nanotubes present in the matrix. As mentioned previously, the resolution of optical microscopy technique limits discerning the information, therefore complimentary higher resolution FESEM technique has been used in this study, and the results will be discussed in the later section. The results presented in Figures 4 and 5 strongly suggest the benefit of using MF and PSM in combination to deagglomerate carbon nanotubes in epoxy mixture over the PSM, or US processing stand-alone methods.

Among the samples characterized by optical microscopy, MF + PSM processed sample showed the most deagglomerated MWCNTs dispersed in epoxy and it was found to be nearly similar to MF processed sample. US + PSM processed sample showed a higher degree of deagglomeration compared with PSM processed sample. US processed sample showed

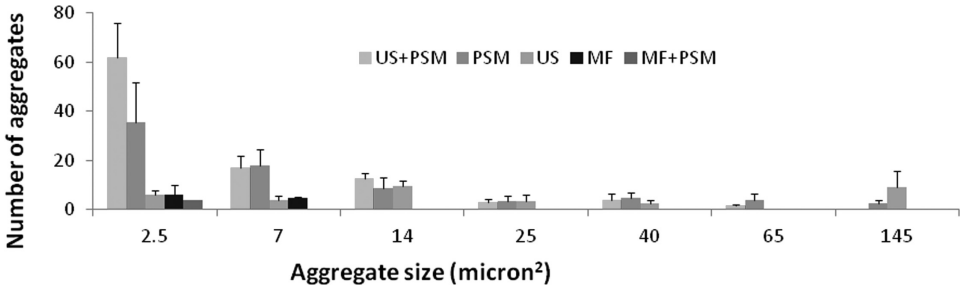

FIGURE 5 Aggregate size distribution of pristine MWCNT/epoxy composites processed using different methods.

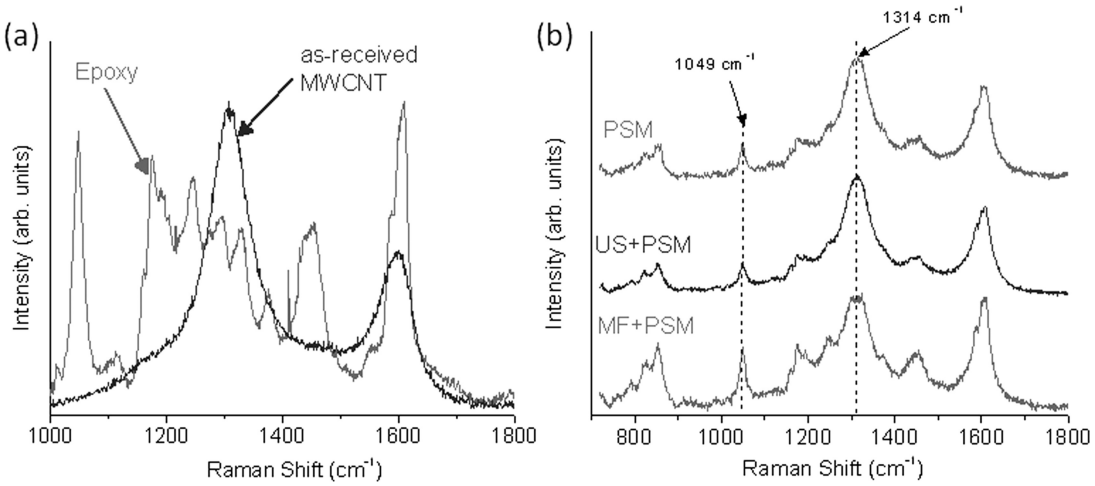

FIGURE 6 (a) Raman spectra of as-received MWCNTs and cured epoxy (no MWCNT). (b) Comparison of representative Raman spectra of PSM, US + PSM, and MF + PSM composites. All composite spectra show Raman features of both MWCNTs and the epoxy matrix. The ratio of the Raman intensities at 1314 and 1049 cm^{-1} (I_{1314}/I_{1049}) can be used to evaluate the amount and the dispersion of MWCNTs in the epoxy.

macroaggregates of MWCNT bundles in epoxy resin. The latter sample was not investigated further because macroaggregates ($> 100\ \mu m^2$) could serve as defects in crosslinked epoxy and can deleteriously impact mechanical properties.[19] Therefore, our next level of characterization was centered around MF + PSM, US + PSM, and PSM processed samples.

Raman Spectroscopy and Raman Mapping

Since Raman imaging resolution is at a scale of few micrometers, only information about large-scale spatial distribution of MWCNTs in the nanocomposite can be obtained. We analyzed the Raman intensity ratio between MWCNTs and the epoxy matrix to provide information about distribution (agglomerations or other inhomogeneities) of MWCNTs in the epoxy matrix that cannot be visually detected. When comparing various composites processed using various processing methods, Raman analysis allows to study changes in the distribution of the MWCNTs as it relates to processing method. If factors, such as MWCNT concentration and random orientation, are assumed to remain the same for the different composites, quantification of the intensity ratio should provide qualitative measure of MWCNT dispersion in the composite. Figure 6(a) shows the Raman spectra of the as-received MWCNTs and the pristine epoxy, recorded using 780-nm laser excitation. The Raman spectrum of the MWCNTs exhibits two distinct features centered at ~1314 and 1600 cm^{-1}, referred to as D band and G band, respectively. The G band originates from the in-plane tangential stretching of the carbon-carbon bonds, whereas the D band is a double-resonant Raman feature resulting from the presence of defects and structural disorder in the MWCNTs.[47] The Raman spectrum of the epoxy is more complex and shows several peaks in the wavenumber range 700–1800 cm^{-1}, some of which directly overlap with the D and G bands of the MWCNTs.

Three representative Raman spectra of the PSM, US + PSM, and MF + PSM composites are shown in Figure 6(b). Each Raman spectrum exhibits the characteristic features of both MWCNTs and epoxy matrix. The intensity ratio between Raman peaks of the two composite components can be used to evaluate the amount and the dispersion of the MWCNTs within the epoxy. In this study, we selected the ratio between Raman intensities measured at 1314 and 1049 cm^{-1}, herein referred to as I_{1314}/I_{1049}, to evaluate the dispersion of the MWCNTs. While the 1049 cm^{-1} feature can primarily be ascribed to the epoxy matrix [see Fig. 6(a)], the Raman peak at 1314 cm^{-1} contains contributions from both epoxy and MWCNTs. According to Figure 6(a), an I_{1314}/I_{1049} ratio of ~0.5 would represent pure epoxy with no MWCNTs, whereas an I_{1314}/I_{1049} ratio of ~25.0 would indicate pure MWCNTs. To analyze the amount and the dispersion of MWCNTs in the various composites, we recorded Raman images of the I_{1314}/I_{1049} ratio for all samples over a 300 × 300 μm area (Fig. 7). The color scale of I_{1314}/I_{1049} was set to a range of 2–9, in which black (2) and red (9) represent the lowest and highest MWCNT content, respectively. I_{1314}/I_{1049} values above 9 therefore all appear as red, while values below 2 all appear as black. According to the data in Figure 7, composites PSM [Fig. 7(a)] and US + PSM [Fig. 7(c)] have the highest MWCNT content, as compared with MF + PSM [Fig. 7(b)], whereas the PSM processed sample exhibits larger inhomogeneities in the distribution of the MWCNTs.

To evaluate adequately, the dispersion of the MWCNTs in each sample, we re-plotted the I_{1314}/I_{1049} data, assigning each Raman image a separate color scale based on the 5% (black) to 95% (red) interval of the measured I_{1314}/I_{1049} values (Fig. 8). The MF + PSM sample [Fig. 8(b)] exhibits the best dispersion and with an I_{1314}/I_{1049} range of ~2.55–3.70 ($\Delta = 1.15$), appears to be the most homogeneous composite over the analyzed sample area (~300 × 300 μm). The

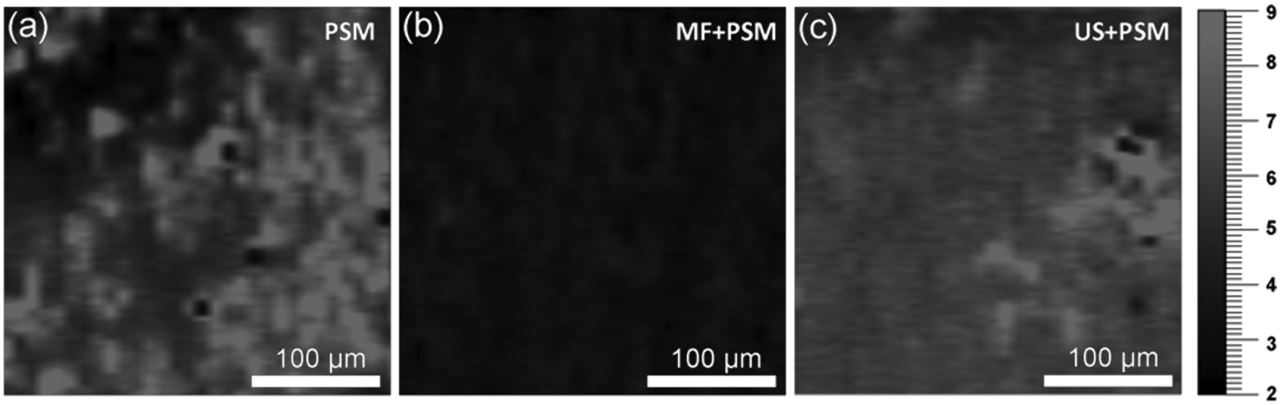

FIGURE 7 Raman intensity ratio (I_{1314}/I_{1049}) image of the PSM (a), MF + PSM (b), and US + PSM (c) composites. The color scale was normalized such that black represents $I_{1314}/I_{1049} \leq 2$ and red represents $I_{1314}/I_{1049} \geq 9$.

I_{1314}/I_{1049} value of the US + PSM sample ranges from 4.80 to 7.75 ($\Delta = 2.95$). The PSM sample [Fig. 8(a)] shows an I_{1314}/I_{1049} range of ~2.75–8.95 ($\Delta = 6.20$) and is therefore the least homogenous composite, among the samples studied. These results are in good agreement with the optical micrographs presented in Figure 4.

Tensile Testing

Tensile testing was performed on dog bone specimens prepared by three different processing methods namely PSM, MF + PSM, and US + PSM using MTS tensile tester. Figure 9 shows the average tensile strength of composite and pristine epoxy specimens. A comparison of the average tensile strengths showed that the samples processed using MF + PSM method have about 15% higher tensile strength than neat resin, whereas the sample processed using PSM or US + PSM exhibits about 15% lower tensile strength compared with pristine epoxy resin. This suggests that the state of dispersion of the MWCNT agglomerates in epoxy resin as evaluated by optical microscopy and micro Raman spectroscopy does influence the bulk mechanical properties of the nanocomposites.

To examine whether there were statistically significant differences in the average tensile strength data due to the various preparation methods, an analysis of significance (t-test) was used. We calculated the confidence level (probability) at which the mean strength of composite specimen processed using various preparation methods are indeed significantly different. A description using t-test has been provided along with Table 1S as part of Supporting Information. For this study, any confidence level below 90% was equivalent to no statistically significant difference. The addition of MWCNTs and processing by PSM or US significantly decreased the strength of the epoxy nanocomposite compared with pure epoxy resin. While the addition of 0.5 wt % MWCNTs and processing by MF + PSM did significantly increase the strength of the epoxy resin. However, the mean strength of epoxy samples containing MWCNTs processed using US + PSM or PSM was not statistically significant. These results suggest that the combination of MF and PSM is an efficient approach to improve MWCNTs dispersion in epoxy and thus improve the strength of nanocomposite.

Scanning Electron Microscopy

To understand how dispersion of MWCNTs can affect the fracture behavior of nanotubes, SEM examination of fractured surfaces of the MWCNT/epoxy nanocomposites were performed. Figure 10 shows the SEM images of (a) pristine MWCNTs, (b) PSM processed nanocomposite, (c) US + PSM processed nanocomposites, and (d) MF + PSM processed nanocomposite. For reference, we show the SEM image of

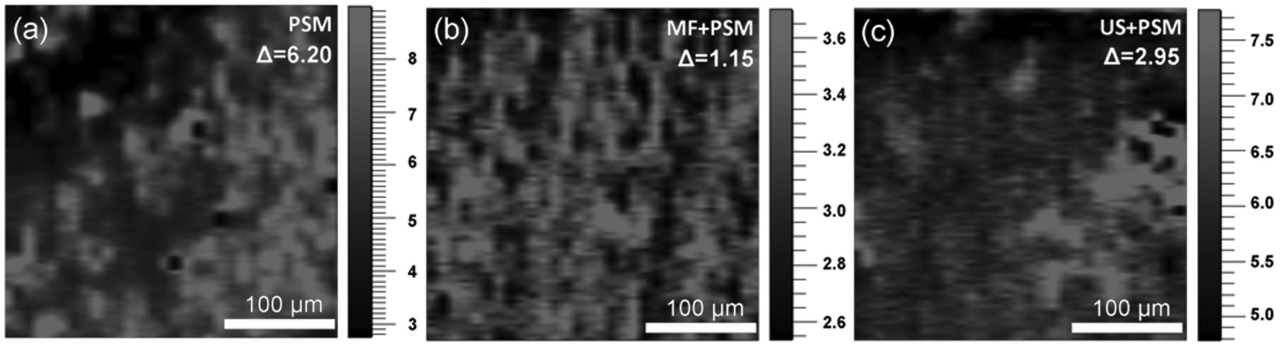

FIGURE 8 Raman intensity ratio (I_{1314}/I_{1049}) image of the PSM (a), MF + PSM (b), and US + PSM (c) composites. The color scale was normalized such that black represents 5% of the maximum I_{1314}/I_{1049} and red represents 95% of the maximum I_{1314}/I_{1049} of each sample.

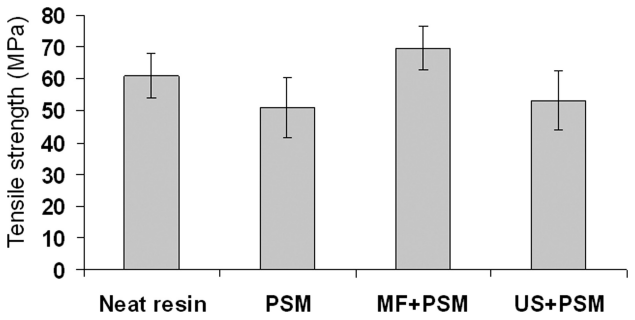

FIGURE 9 Tensile strength data (MPa) for MWCNTs/epoxy nanocomposites processed by different methods.

pristine MWCNTs deposited on a silicon wafer and the fine structures corresponding to the individual nanotubes. In the SEM images of fractured sample of processed MWCNT/epoxy composite, we clearly observe thin structures showing MWCNTs. The hairy structures exist either as isolated oriented thin clusters, agglomerates, or individual nanotubes in the bulk epoxy matrix. For the PSM processed sample, aggregates of the nanotubes were noticed as shown in Figure 10(b) inset, while for the MF + PSM processed sample smaller sized aggregates were noticed throughout the matrix [Fig. 10(d) inset]. A close examination of the fractured sample of MF + PSM processed specimen at high magnification, showed better dispersion of nanotubes throughout the matrix. Additionally, the individual nanotubes in the fractured sample of MF + PSM processed specimen [Fig. 10(d)] showed actual "break" which appear as bright spots at the end of the nanotubes indicated by dotted red arrows.[15] Our results are consistent with Gonzalez et al.; Gonzalez reported that the block copolymer (pluronic) wrapped SWCNTs when well dispersed in the epoxy matrix show as "bright dots" in the SEM images of fractured surfaces, which were interpreted by the authors as "broken out" CNTs and was noted as the reason for mechanical property improvement. However, the fractured sample of PSM processed specimen showed poor dispersion of nanotubes throughout the matrix and "pull-out" phenomena as seen by curled tubes in the image as indicated by solid red arrows. Song et al. reported noticing curly tube structures in the fractured surfaces of MWCNT/epoxy nanocomposites when imaged by FESEM for poorly reinforced CNT nanocomposite host matrix.[19] High magnification SEM of US + PSM sample shown in Figure 10(c) indicated both pull out and broken nanotubes, which suggest a combination of fracture mechanisms influencing the mechanical properties of the nanocomposites. These results compliment the earlier findings from optical microscopy and Raman microscopy that MF and PSM processing in

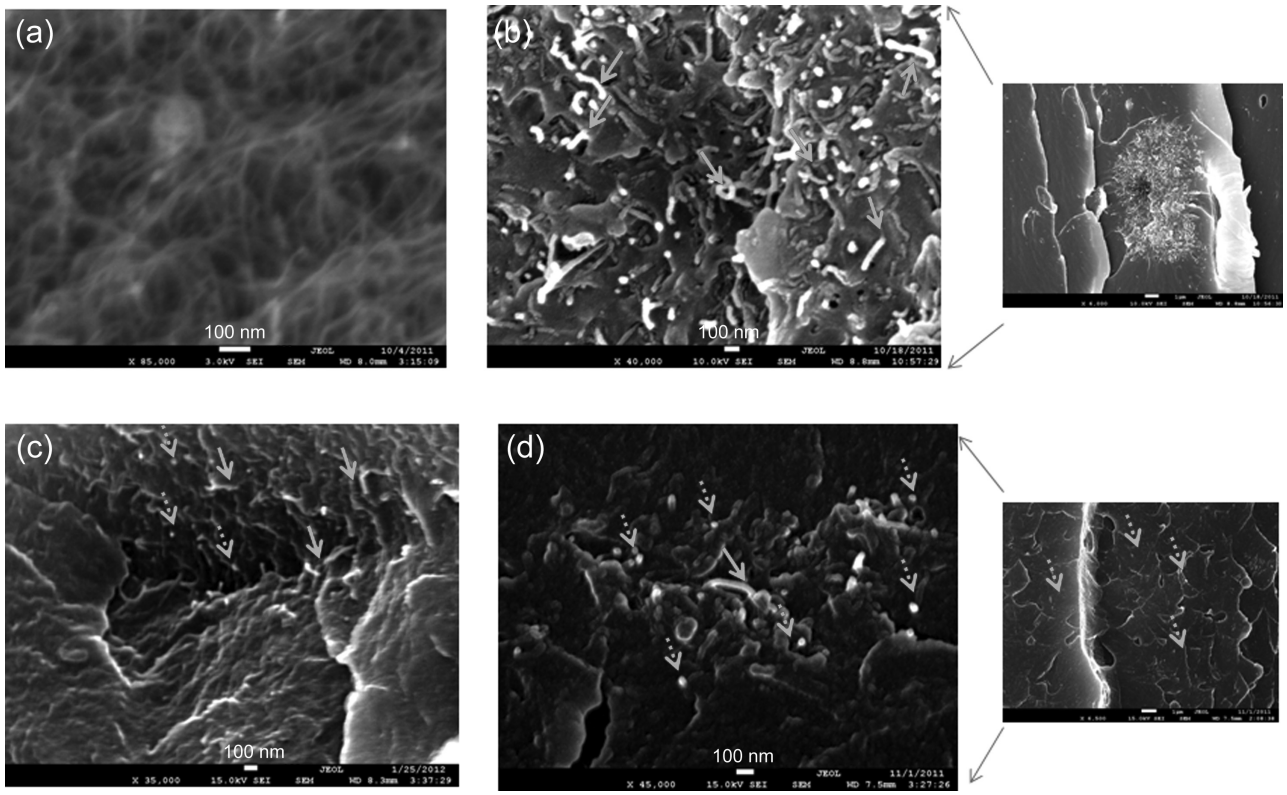

FIGURE 10 FESEM image of (a) pristine MWCNT and the images of fractured surfaces of pristine MWCNT/epoxy processed by: (b) TM, (c) US + PSM, and (d) MF + PSM. Red solid arrows represent "pulled out" CNTs seen as curled tubes and red dotted arrows represent as "broken" MWCNTs, which can be seen as bright dots in the SEM images. All scale bars shown at the bottom frame in each of the images are at 100 nm scale. Figures (b) and (d) have also been shown at lower magnification (1 μm scale bar) in the inset to present the state of CNT aggregation.

TABLE 1 Effect of Processing Method on Thermal Stability and Onset of Degradation Temperature of Epoxy-MWCNT Nanocomposite

Material	Onset of degradation temperature (5% weight loss)
Neat epoxy	367 ± 0.5 °C
Pristine PSM	362 ± 0.6 °C
Pristine MF + PSM	367 ± 0.4 °C

combination yields better-dispersed samples than PSM and US + PSM processed sample.

Thermogravimetric Analysis

The thermal stability of polymeric materials is defined by parameters such as the onset decomposition temperature (T_d), which is defined as the temperature at which 5% mass loss occurs in the sample. To determine T_d, the thermal stability of epoxy and epoxy nanocomposites was evaluated by TGA. A repeat of three TGA measurements was carried out for each sample and an average with standard deviation was reported in Table 1. Table 1 summarizes the onset decomposition of cured epoxy and epoxy nanocomposites processed using PSM and MF + PSM methods. A modest decrease (5 °C) in the onset of degradation temperature in the PSM processed nanocomposite sample compared with pristine epoxy resin was noticed. This indicates that the MWCNT aggregates present in the PSM processed sample may act as inhibitors or barriers to the curing of epoxy and cause the observed lower temperature at which the 5% weight loss occurs. These results are consistent with the description presented in the review paper by Bikiaris and Tao in which pristine MWCNTs were described as exhibiting poor affinity towards epoxy resin compared with functionalized MWCNTs.[48,49] Our TGA results support optical, Raman and SEM observations of PSM processed samples and also reduction of tensile strength over the neat epoxy resin. However, the sample processed by MF + PSM showed no increase in onset of degradation temperature compared with that of neat resin. Again, our TGA results support dispersion resulting from the MWCNTs in the polymer matrix as obtained by optical microscopy Raman spectroscopy and SEM, where better dispersion of MWCNTs cause limited interference during curing of epoxy resin.

CONCLUSIONS

Processing methods greatly influence dispersion of MWCNTs in epoxy resin and thus the performance of the resulting nanocomposite. A better dispersion of nanotubes in epoxy was achieved by a combination of microfluidic processing and planetary shear mixing. The extent of dispersion of MWCNT agglomerates in the epoxy was quantified by optical microscopy combined with image analysis. The results of optical image analysis data were found to corroborate with Raman images derived from I_{1314}/I_{1049} ratio and high resolution FESEM examination of fractured surface of the obtained nanocomposite. Improvement in tensile strength was noted when using the MF + PSM processing method compared with pristine epoxy resin. An improved dispersion of nanotubes in MF + PSM processed samples resulted in an increase in tensile strength of the pristine resin by 15% while the poor dispersion of nanotubes in PSM processed samples resulted in reduction in the tensile strength of the resin. The influence of dispersion quality of MWCNTs in epoxy resin on thermal properties was studied by TGA measurements. Weight loss characterization of PSM processed samples revealed that poorly dispersed samples have marginally (5 °C) lower onset degradation temperature than pristine samples. Detailed studies are underway to evaluate the effect of various processing methods on dispersion of functionalized MWCNTs in epoxy resin and its impact on the overall mechanical and thermal properties of nanocomposites.

ACKNOWLEDGMENTS

The authors gratefully acknowledge financial support from US Army Research Office grant through Institute for Soldier Nanotechnologies at Massachusetts Institute of Technology, Cambridge, MA, and from the Research Initiative Program of the Naval Postgraduate School, Monterey, CA. Ian Gunniss at Microfluidics Inc, Newton, MA is acknowledged for processing the samples by Microfluidizer. They are grateful to Thinky Corporation, USA in loaning the equipment for processing the samples. Authors also appreciate assistance of James Griffin in collecting FESEM images at NSF sponsored Nanomaterials Center Howard University. Quentin Roby and Dajanae Cooper (HU undergraduates) are acknowledged for their assistance with sample preparation and sample characterization. Finally, the authors would like to acknowledge the assistance from Maraizu Ukaegbu and Dr. Charles Hosten of Howard University in showing the viability of Raman spectroscopy in mapping MWCNT dispersion in epoxy nanocomposite.

REFERENCES AND NOTES

1 J. R. Fried, Polymer Science and Technology; Prentice Hall: New Jersey, **1995;** p 4.

2 C. Chen, T. B. Tolle, *J. Polym. Sci. Part B: Polym. Phys.* **2004,** *42*, 3981–3986.

3 N. Dilsiz, E. Ebert, W. Weisweiler, G. Akovali, *J. Colloid Interface Sci.* **1995,** *170*, 241–248.

4 J. N. Coleman, U. Khan, W. J. Blau, Y. K. Gunâko, *Carbon* **2006,** *44*, 1624.

5 R. Kotsilkova, D. Fragiadakis, P. Pissis, *J. Polym. Sci. Part B: Polym. Phys.* **2005,** *43*, 522–533.

6 M. M. Ruiz, J. Y. Cavaillé, A. Dufresne, C. Graillat, J.-F. Gérard, *Macromol. Symp.* **2001,** *169*, 211–222.

7 D. Raghavan, C. Chenggang, In Advances in Polymer Nanocomposites Technology; V. Mittal, Ed.; Thermally Stable Polymer Nanocomposites; Nova Publishers, **2010;** Chapter 7, p 1–26.

8 E. Camponeschi, B. Florkowski, R. Vance, G. Garrett, H. Garmestani, R. Tannenbaum, *Langmuir* **2006,** *22*, 1858–1862.

9 A. Eitan, K. Jiang, D. Dukes, R. Andrews, L. S. Schadler, *Chem. Mater.* **2003,** *15*, 3198–3201.

10 S. Rana, R. Alagirusamy, M. A. Joshi, *J. Reinforced Plast. Compos.* **2009,** *28*, 461–487.

11 P. R. Thakre, Y. Bisrat, D. C. Lagoudas, *J. Appl. Polym. Sci.* **2010,** *116*, 191–202.

12 J. Zhu, H. Peng, F. Rodriguez-Macias, J. L. Margrave, V. N. Khabashesku, A. M. Imam, K. Lozano, E. V. Barrera, *Adv. Functional Mater.* **2004,** *14*, 643–648.

13 F. H. Gojny, M. H. G. Wichmann, B. Fiedler, K. Schulte, *Compos. Sci. Technol.* **2005,** *65*, 2300–2313.

14 F. H. Gojny, M. H. G. Wichmann, U. Kopke, B. Fiedler, K. Schulte, *Compos. Sci. Technol.* **2004,** *64*, 2363–2371.

15 J. M. Gonzalez-Dominguez, A. Anson-Casaos, A. M. Diez-Pascual, B. Ashrafi, M. Naffakh, D. Backman, H. Stadler, A. Johnston, M. Gomez, M. T. Martinez, *ACS Appl. Mater. Interfaces* **2011,** *3*, 1441–1450.

16 K.-T. Lau, M. Lu, C.-K. Lam, H.-Y. Cheung, F.-L. Sheng, H.-L. Li, *Compos. Sci. Technol.* **2005,** *65*, 719–725.

17 Y. Martinez-Rubi, B. Ashrafi, J. Guan, C. Kingston, A. Johnston, B. Simard, V. Mirjalili, P. Hubert, L. Deng, R. L. Young, *ACS Appl. Mater. Interfaces* **2011,** *3*, 2309–2317.

18 R. Hollertz, S. C. H. Gutmann, T. Geiger, F. A. Nüesch, B. T. T. Chu, *Nanotechnology* **2011,** *22*, 125702.

19 Y. S. Song, J. R. Youn, *Carbon* **2005,** *43*, 1378–1385.

20 E. Dujardin, T. W. Ebbesen, A. Krishnan, M. M. J. Treacy, *Adv. Mater.* **1998,** *10*, 1472–1475.

21 S. Banerjee, T. Hemraj-Benny, S. S. Wong, *Adv. Mater.* **2005,** *17*, 17–29.

22 R. Blake, Y. K. Gunko, J. Coleman, M. Cadek, A. Fonseca, J. B. Nagy, W. J. Blau, *J. Am. Chem. Soc.* **2004,** *126*, 10226–10227.

23 R. E. Gorga, K. K. S. Lau, K. K. Gleason, R. E. Cohen, *J. Appl. Polym. Sci.* **2006,** *102*, 1413–1418.

24 F. Liang, A. K. Sadana, A. Peera, J. Chattopadhyay, Z. Gu, R. H. Hauge, W. E. Billups, *Nano Lett.* **2004,** *4*, 1257–1260.

25 D. Mao, *SAMPE Conf. Proc.* **2009,** *54*, 1–9.

26 J. Wang, Z. Fang, A. Gu, L. Xu, F. Liu, *J. Appl. Polym. Sci.* **2006,** *100*, 97–104.

27 S. Wang, Z. Liang, T. Liu, B. Wang, C. Zhang, *Nanotechnology* **2006,** *17*, 1551.

28 S. Osswald, M. Havel, Y. Gogotsi, *J. Raman Spectros.* **2007,** *38*, 728–736.

29 J. A. Kim, D. G. Seong, T. J. Kang, J. R. Youn, *Carbon* **2006,** *44*, 1898–1905.

30 P. M. Ajayan, L. S. Schadler, C. Giannaris, A. Rubio, *Adv. Mater.* **2000,** *12*, 750–753.

31 K. T. Lau, M. Lu, C. Lam, H. Cheung, F. L. Sheng, H. L. Li, *Compos. Sci. Technol.* **2005,** *65*, 719.

32 F. H. Gojny, M. H. G. Wichmann, U. Kopke, B. Fiedler, K. Schulte, *Compos. Sci. Technol.* **2004,** *64*, 2363.

33 E. T. Thostenson, T.-W. Chou, *Carbon* **2006,** *44*, 3022–3029.

34 P. R. Thakre, Processing and characterization of carbon nanotubes reinforced epoxy resin based multi-scale multi-functional composites. PhD Thesis, Texas A and M Univ., College Station, TX, USA, **2009**.

35 T. Panagiotou, J. M. Bernard, S. V. Mesite, In Deagglomeration and Dispersion of Carbon Nanotubes Using Microfluidizer® High Shear Fluid Processors; NSTI-Nanotech, Boston, MA, **2008;** pp 39–42.

36 Microfluidics technology. Available at: http://www.microfluidicscorp.com/index.php?option=com_content&view=article&id=49&Itemid=180. Accessed on October 16, 2012.

37 G. R. Kasaliwal, S. Pegel, A. Goldel, P. Potschke, G. Heinrich, *Polymer* **2010,** *51*, 2708–2720.

38 C. Park, P. Lillehei, Optical, Electron and Probe Microscopy; National Institute of Standards and Technology: Gaithersburg, MD, **2008;** pp 55–72.

39 M. Mu, S. Osswald, Y. Gogotsi, K. I. Winey, *Nanotechnology* **2009,** *20*, 335703.

40 T. E. Chang, L. R. Jensen, A. Kisliuk, R. B. Pipes, R. Pyrz, A. P. Sokolov, *Polymer* **2005,** *46*, 439–444.

41 M. D. Frogley, D. Ravich, H. D. Wagner, *Compos. Sci. Technol.* **2003,** *63*, 1647–1654.

42 S. L. Ruan, P. Gao, X. G. Yang, T. X. Yu, *Polymer* **2003,** *44*, 5643–5654.

43 L. S. Schadler, S. C. Giannaris, P. M. Ajayan, *Appl. Phys. Lett.* **1998,** 3842.

44 F. Du, R. C. Scogna, W. Zhou, S. Brand, J. E. Fischer, K. I. Winey, *Macromolecules* **2004,** *37*, 9048–9055.

45 Planetray Centrifugal mixer – ARE 310. Available at: www.thinkyusa.com.

46 Microfluidizer processor webinar prentation. Available at: http://www.microfluidicscorp.com/index.php?option=com_content&view=article&id=77&Itemid=182.

47 M. S. Dresselhaus, G. Dresselhaus, R. Saito, A. Jorio, *Phys. Rep.* **2005,** *409*, 47–99.

48 D. Bikiaris, *Thermochim. Acta* **2011,** *523*, 25–45.

49 K. Tao, S. Yang, J. C. Grunlan, Y.-S. Kim, B. Dang, Y. Deng, R. L. Thomas, B. L. Wilson, X. Wei, *J. Appl. Polym. Sci.* **2006,** *102*, 5248–5254.